Journal of Catalysis 258 (2008) 52–60

Contents lists available at ScienceDirect

Journal of Catalysis

www.elsevier.com/locate/jcat

Enhancing the catalytic performance of Pt/ZnO in the selective hydrogenation of cinnamaldehyde by Cr addition to the support

E.V. Ramos-Fernández [a], A.F.P. Ferreira [b], A. Sepúlveda-Escribano [a,*], F. Kapteijn [b], F. Rodríguez-Reinoso [a]

[a] Departamento de Química Inorgánica, Universidad de Alicante, Apartado 99, E-03080 Alicante, Spain
[b] Catalysis Engineering, DelftChemTech, Delft University of Technology, Julianalaan, 136, 2628 BL Delft, Netherlands

ARTICLE INFO

Article history:
Received 22 January 2008
Revised 8 April 2008
Accepted 29 May 2008
Available online 1 July 2008

Keywords:
Cinnamaldehyde hydrogenation
Pt
Cr–ZnO
SMSI

ABSTRACT

An enhancement of the catalytic performance of platinum in the liquid phase hydrogenation of cinnamaldehyde has been achieved by modifying a ZnO support by addition of Cr(III) cations. The addition of chromium improves the structural properties of the support (larger surface area) and increases its reducibility, and resulted in a better Pt dispersion. The presence of chromium in the support enhanced the overall catalytic activity, and improved the high selectivity towards the unsaturated alcohol. The increase of the reduction temperature from 473 K to 623 K produces an impressive decrease in the turnover frequency for Pt/ZnO, whereas this value remains practically unmodified for Pt/Cr–Zn. The higher reduction temperature reduces the overall activity in both catalysts, but improves selectivity towards the unsaturated alcohol. The present 5 wt% Pt/Cr–ZnO catalyst showed the best results (in terms of selectivity) published until now without use of reaction promoters. The improved performance of this catalyst is ascribed to an adequate metal–support interaction and to the higher reducibility of the support that opens the possibility of alloy formation.

1. Introduction

The search for chemoselective catalysts is an issue of great interest for the production of many pharmaceutical, agrochemicals, and fragrance compounds [1–3]. Thus, the hydrogenation of organic substrates containing several unsaturated functional groups has been attracting a lot of interest for fundamental research in catalysis. The selective hydrogenation of the carbonyl bond in α,β-unsaturated aldehydes with supported metal catalysts is still a challenge in heterogeneous catalyst. The selective reduction can be achieved by means of properly designed organometallic catalysts, through a Meerwein–Ponndorf–Verley reaction with alcohols as reducing agents and solid Lewis acids as catalysts [4–6]. However, the selective hydrogenation of the carbonyl bond in the presence of an olefinic bond is not an easy task with metallic catalysts, as the C=C bond hydrogenation is favoured both from thermodynamic and kinetics considerations [7,8]. Therefore, it is necessary to modify the intrinsic behaviour of the metal in order to increase the selectivity toward the formation of the desired unsaturated alcohol.

The metal promotion can be achieved by weakening the C=O bond and/or by avoiding the adsorption through C=C bond, and there are several ways of obtaining one or both of these effects. It is well known that the addition of a second, more electropositive metal, like iron [9], tin [10–12] or zinc [13], to supported platinum enhances it selectivity. This has been explained on the basis of alloy formation, which results in the weakening of the adsorption through the olefinic bond and in the presence of acid Lewis centres (the more electropositive metal atoms) that interact with the oxygen atom in the carbonyl bond and favours its hydrogenation [11,14].

Also, the choice of the support can play an important role. The support can affect the catalytic behaviour of the noble metal through several mechanisms. Thus, it has been shown that the selectivity towards the hydrogenation of the carbonyl bond in cinnamaldehyde can be increased by encapsulating Pt particles in Y-type zeolite [15,16]. In this case, it has been claimed that molecular constraints in the zeolite micropores favour the adsorption of the cinnamaldehyde molecule on the metal particles through the carbonyl bond, this facilitating its hydrogenation. However, diffusional limitations induced by the microporous structure yielded low reaction rates [16]. Electronic effects due to the support can also be used. In this way, Giroir-Fendler et al. [17] compared the behaviour of group VIII noble metals supported on activated carbon and graphite in the hydrogenation of cinnamaldehyde, and observed that the graphite-supported systems were more selective, under the same experimental conditions. This higher selectivity was explained on the basis of an electron transfer from the graphitic support to the metal particles located at the edges of the basal planes. The increased charge density on the metal particles

* Corresponding author. Fax: +34 965 90 34 54.
E-mail address: asepul@ua.es (A. Sepúlveda-Escribano).

0021-9517/$ – see front matter
doi:10.1016/j.jcat.2008.05.025

would decrease the probability of adsorption via the C=C bond, thus hindering its hydrogenation. More recently, several studies have dealt with the promotion of platinum particles by graphitic supports such as carbon nanotubes and nanofibres, for which the promotion effect would be expected to be higher. However, the selectivity values obtained up to now have been relatively low [18,19].

Other interesting supports for achieving promotion in this kind of reactions are partially reducible oxides such as TiO_2 [20–22], ZnO [13,14,23–25] CeO_2 [26–29] or SnO_2 [30,31]. In these cases, the possible interaction of the noble metal with the partially reduced oxide (SMSI: strong metal–support interaction effect) or even with the metal formed upon a reduction treatment, has been proposed to be responsible for the improved selectivity. In the case of zinc oxide, both effects can play a role. When platinum is supported on ZnO, the onset of electronic and ensemble effects is well known [14,23]. The electronic effects are due to free electrons produced upon the partial reduction of ZnO to Zn, these free electrons being donated to Pt [32]. The resulting increase in electron density of Pt enhances its catalytic properties, in terms of selectivity, because the probability of adsorption via the C=C bond is decreased [23]. The reducibility of ZnO can be improved through valence induction by doping the oxide support with cations having a formal charge larger than +2. The addition to the support of an appropriate doping cation in the proper amount can also increase the BET surface area by suppressing the ZnO crystal growth.

This paper reports the effect of the addition of Cr(III) to ZnO on the catalytic behaviour of supported platinum in the liquid phase selective hydrogenation of cinnamaldehyde.

2. Experimental

2.1. Catalysts preparation

Two catalyst supports were prepared by a homogeneous co-precipitation method: pure ZnO (S_{BET}: 5 m^2/g) and Cr–ZnO (Cr/Zn atomic ratio of 0.12, S_{BET}: 10 m^2/g). An aqueous solution (pH 9) containing $Zn(NO_3)_2{\cdot}H_2O$, $CO(NH_2)_2$ and, for the Cr–ZnO support also $Cr(NO_3)_3{\cdot}9H_2O$, was strongly stirred and then heated up to 365 K. The precipitate formed was centrifuged and calcined in air at 773 K for 2 h with a heating rate of 10 K/min. For catalyst preparation, the supports were immersed into an aqueous solution of $H_2PtCl_6{\cdot}6H_2O$ of the adequate concentration as to achieve a Pt loading of 5 wt%, and stirred for 24 h. Then, the excess of solvent was removed by evaporation in a rotary evaporator at 363 K and the obtained solids were calcined in air at 773 K for 2 h with a heating rate of 10 K/min. The catalysts obtained were labelled as Pt/ZnO and Pt/Cr–ZnO.

2.2. Supports characterisation

The textural properties of the prepared materials were determined by nitrogen adsorption at 77 K on a Coulter Omnisorp 610 system. Before measurements, the samples were dried at 383 K for 12 h and out-gassed at 523 K under vacuum for 4 h. Their surface areas were calculated following the BET method in the relative pressure range from 0.05 to 0.25.

The X-ray diffraction patterns of the supports were obtained with a JSO Debye-Flex 2002 system, from Seifert, fitted with a Cu cathode and a Ni filter, and using a 2°/min scanning rate. The room temperature Raman spectra were recorded on a Raman-laser spectrometer using a 514.5 nm line of an argon-ion laser.

2.3. Catalysts characterisation

Conventional TEM analysis was carried out with a JOEL model JEM-210 electron microscope working at 200 kV and equipped with an INCA Energy TEM 100 analytical system and a SIS Mega-View II camera. The samples reduced at 623 K were suspended in methanol and placed on copper grids with a holey-carbon film support.

Temperature-programmed reduction (TPR) measurements were carried out in a U-shaped quartz reactor, using a 5% H_2/He gas flow of 50 cm^3/min and 100 mg of catalyst, with a heating rate of 10 K/min. The hydrogen consumption was monitored by mass spectrometry.

X-ray photoelectron spectra (XPS) were acquired with a VG-Microtech Multilab 3000 spectrometer equipped with a hemispherical electron analyser and a Mg$K\alpha$ ($h = 1253.6$ eV, 1 eV = 1.6302×10^{-19} J) 300-W X-ray source. The powder samples were pressed into small Inox cylinders and then mounted on a sample rod placed in a pretreatment chamber and reduced in flowing H_2 for 1 h at 473 and 623 K before being transferred to the analysis chamber. Before recording the spectra, the sample was maintained in the analysis chamber until a residual pressure of ca. 5×10^{-7} N/m^2 was reached. The spectra were collected at pass energy of 50 eV. The intensities were estimated by calculating the integral of each peak, after subtraction of the S-shaped background, and by fitting the experimental curve to a combination of Lorentzian (30%) and Gaussian (70%) lines. All binding energies (BE) were referenced to the C 1s line at 284.6 eV, which provided binding energy values with an accuracy of ±0.2 eV. The surface atomic ratios were estimated from the integrated intensities corrected by the atomic sensitivity factors [33].

The CO chemisorption experiments were carried out in a manometric equipment. Before CO chemisorption, the samples were reduced at 473 K and 623 K under flowing hydrogen for 1 h, and then cleaned up with a helium flow (50 ml/min) for 1 h at the same temperature. Chemisorption data were collected by sequentially introducing small doses (1–10 μmol) of CO (99.5%, with further purification, Air Liquide) onto the sample at 298 K until it became saturated. The amount of gas adsorbed (μmol) was determined manometrically from the dosis, equilibrium pressures, and the system's volumes and temperatures. The time required for the pressure to equilibrate in the cell after each dosis was approximately 40 min.

2.4. Catalytic tests

The liquid phase hydrogenation of cinnamaldehyde was carried out in a 300 ml stirred autoclave (Biometa, fitted with a system for liquid sampling) at 383 K and at constant pressure of 7 MPa. Pre-reduced catalysts (300 mg) were immersed into 90 ml of solvent (isopropanol 99% previously out-gassed by bubbling a flow of helium). After a first flush with helium and a second one with hydrogen, the temperature was raised to 383 K under 3 MPa of hydrogen to re-active the catalysts. Then, a mixture of substrate (0.5 ml of cinnamaldehyde) and solvent (10 ml) was loaded into the autoclave through a liquid container under a 7 MPa hydrogen pressure. The final cinnamaldehyde concentration was 0.04 mol/l. Zero time was taken at this moment and stirring was switched on. Liquid samples were analysed on a gas chromatograph equipped with a FID detector and a capillary Carbowax column, using helium as carrier gas.

3. Results

3.1. XRD analysis

Fig. 1 shows the XRD patterns of the ZnO and Cr–ZnO supports. For the pure zinc oxide support all the diffraction peaks in the pattern can be assigned to the hexagonal (würtzite-type) ZnO, with lattice constants $a = 3.25$ Å and $c = 5.20$ Å. The comparison of

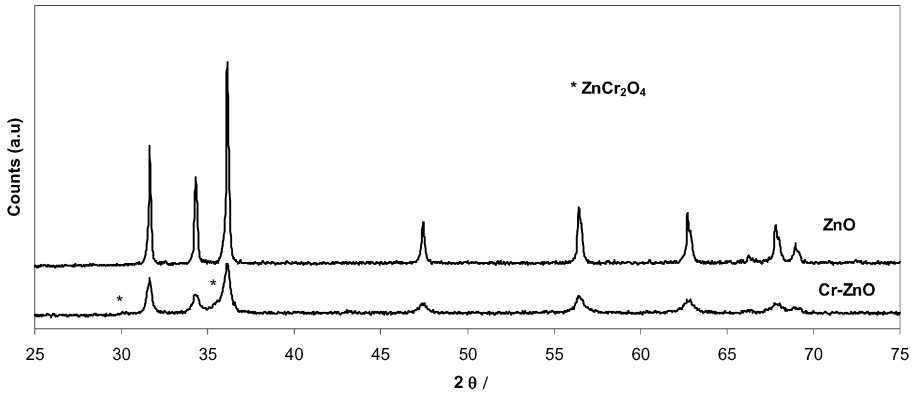

Fig. 1. XRD patterns of the supports.

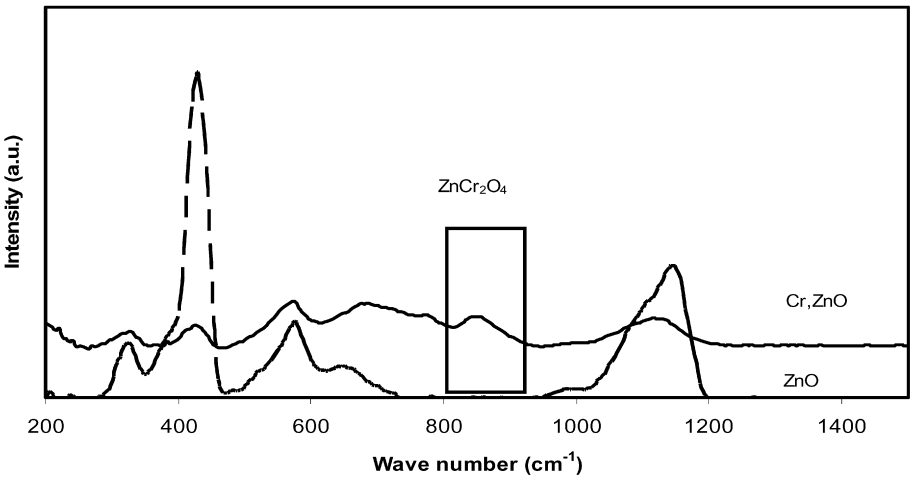

Fig. 2. Raman spectra of the supports.

the observed and standard intensities [34] of the diffraction peaks indicates that there are not preferred orientations. The diffraction peaks are narrow and intense, indicating a high crystallinity. Two crystalline structures can be observed in the XRD pattern of the Cr–ZnO support: hexagonal ZnO and, to a lesser extent, spinel $ZnCr_2O_4$. The crystallinity of the former is poorer for this support, and the wider diffraction peaks indicate a smaller crystallite size. The presence of crystalline Cr_2O_3 was not detected.

3.2. Raman spectroscopy

Raman spectra of the Cr–ZnO and ZnO supports are collected in Fig. 2. The spectra obtained for the pure ZnO support shows several bands, which are assigned to the Raman active mode of the material with würtzite-type structure (ZnO). Thus, the Raman $E_{2(high)}$, $A_{1(LO)}$ and $A_{1(TO)}$ phonon modes at 430, 569, and 383 cm^{-1}, respectively, were clearly observed, this indicating that the ZnO crystals did not show any preferred orientation. The band at 320 cm^{-1} is the second order Raman spectrum arising from zone-boundary phonons 2-E_2 of ZnO [35]. In würtzite structure crystals, stress induced in the crystals affects the E_2 phonon frequency. An increase in the E_2 phonon frequency is ascribed to compressive stress, whereas a decrease in the E_2 phonon frequency is ascribed to tensile stress [35]. The addition to the structure of a second ion with a different atomic radius is considered to be the main factor that would cause lattice distortion in the crystals. It can be seen that after chromium addition, the E_2 phonon frequency is shifted to lower wavenumbers (from 430 cm^{-1} to 425 cm^{-1}), indicating a large tensile stress remaining in the ZnO crystals. The chromium ion radius is very similar to that of Zn(II), so in principle, the shift should be lower. However, the amount of chromium added is very high and this produces a large distortion in the ZnO structure. The broad features between 1025–1150 cm^{-1} are assigned to the two-phonon modes (2-LO), characteristic of this II–IV semiconductor [36]. The spectra for the Cr–ZnO support showed the Raman active modes of würtzite-type structure and a peak centred at 845 cm^{-1}, which is ascribed to the $ZnCr_2O_4$ spinel structure. These findings corroborate those obtained by XRD diffraction, i.e., the presence of a $ZnCr_2O_4$ spinel structure. The decrease in the E_2 phonon frequency demonstrates that the chromium ions are taken part in the ZnO structure forming zinc chromite. No indications of the Cr_2O_3 phase were found.

3.3. Transmission electron microscopy

Fig. 3 shows TEM micrographs obtained for the two catalysts reduced at 623 K. Dark zones are due to platinum particles, whereas lighter parts correspond to the support. Homogeneous particle size distributions have been found in both catalysts, being especially narrower for catalyst Pt/Cr–ZnO. Analysis of a set of high magnification images allowed to obtain the particle size distributions presented in Fig. 4. The particle size distribution for the Pt/ZnO catalyst is centred at 4.1 ± 1.2 nm, whereas for Pt/Cr–ZnO it is centred at 1.7 ± 0.5 nm. The addition of Cr generated a support with larger surface area, this resulting in a better platinum dispersion. The low surface area of ZnO and the relative high platinum loading (5 wt%) caused larger platinum particles to be formed on Pt/ZnO. Catalyst reduced at 473 K showed the same platinum par-

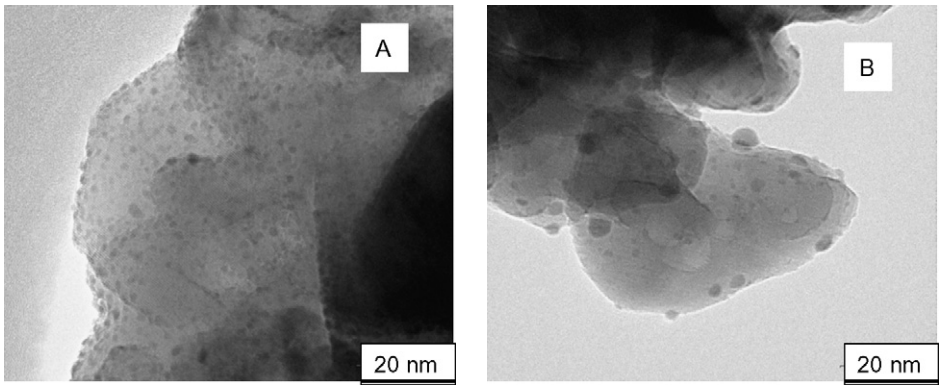

Fig. 3. TEM pictures of catalysts reduced at 623 K: (A) Pt/Cr–ZnO; (B) Pt/ZnO.

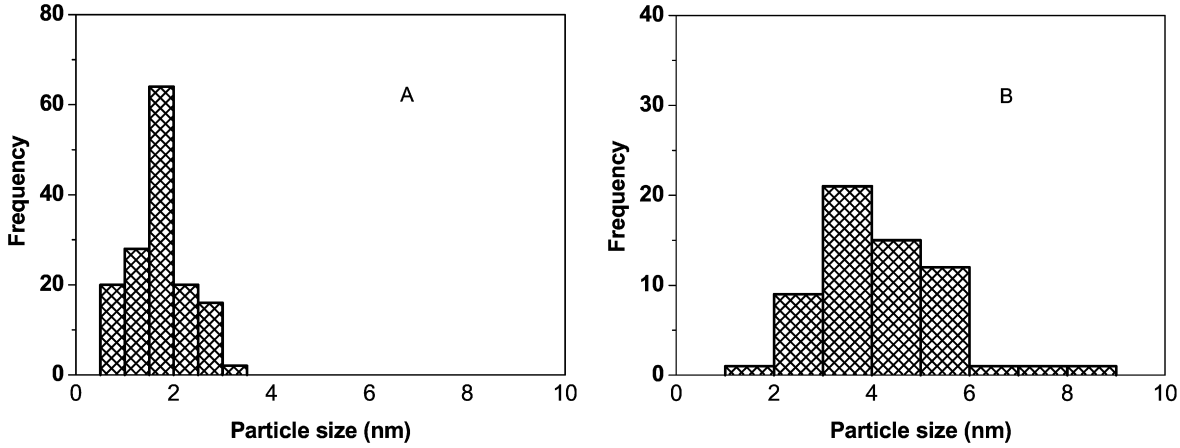

Fig. 4. Size distribution of Pt particles on catalysts reduced at 623 K: (A) Pt/Cr–ZnO, (B) Pt/ZnO.

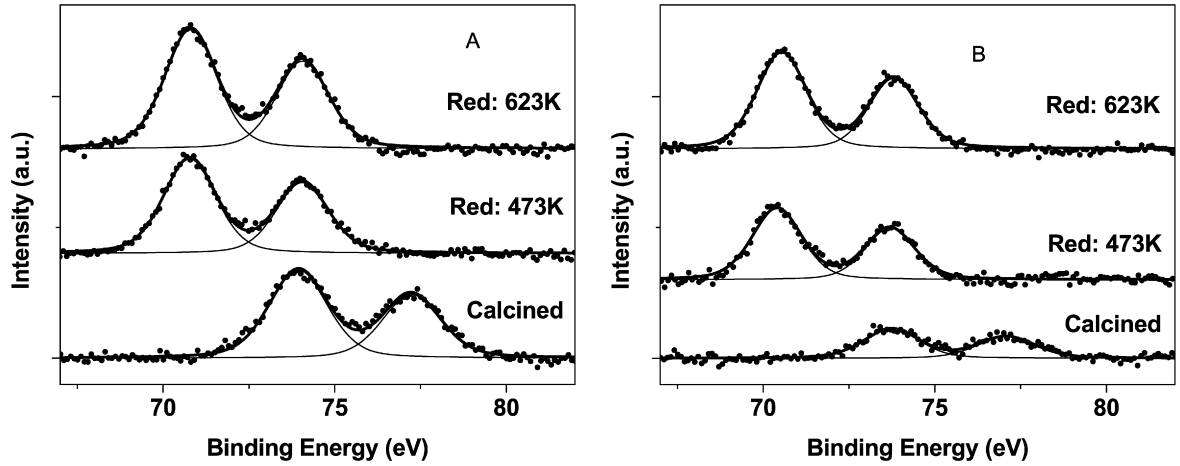

Fig. 5. Pt 4f core-level photoelectron spectra of the Pt/Cr–ZnO catalyst (A) and Pt/ZnO catalysts (B) after reduction and calcination treatments.

ticle size distribution, this indicating that the reduction treatment at 623 K did not result in any sintering of the metal particles.

3.4. X-ray phoelectron spectroscopy

The Pt 4f level X-ray photoelectron spectra for catalyst Pt/ZnO after reduction in flowing hydrogen at 473 K and 623 K are shown in Fig. 5. The calcined unreduced sample presents two peaks at 73.8 eV (level Pt $4f_{7/2}$) and 77.1 eV (level Pt $4f_{5/2}$). Both peaks are unambiguously ascribed to electron deficient Pt(II) species [37–39]. Both peaks shifted to lower binding energies (BE) after the reduction treatment. The peak corresponding to Pt $4f_{7/2}$ level now appears at 70.5 eV, which is characteristic of metallic platinum. The same behaviour was found for catalyst Pt/Cr–ZnO. These results indicate that Pt species are fully reduced even after the reduction treatment at low temperature (473 K).

The O 1s spectrum (not shown) for catalysts Pt/ZnO and Pt/Cr–ZnO both calcined (un-reduced) and after reduction, showed the presence of two oxygen components at BE 530 eV and 531.5 eV. The first peak, centred at 530 eV, corresponds to oxygen taking part in the Zn–O bond, and the second one is ascribed to –OH surface groups [40]. The intensity of the peak at 531.5 eV decreased after the reduction treatments, thus indicating the partial removal of the –OH groups.

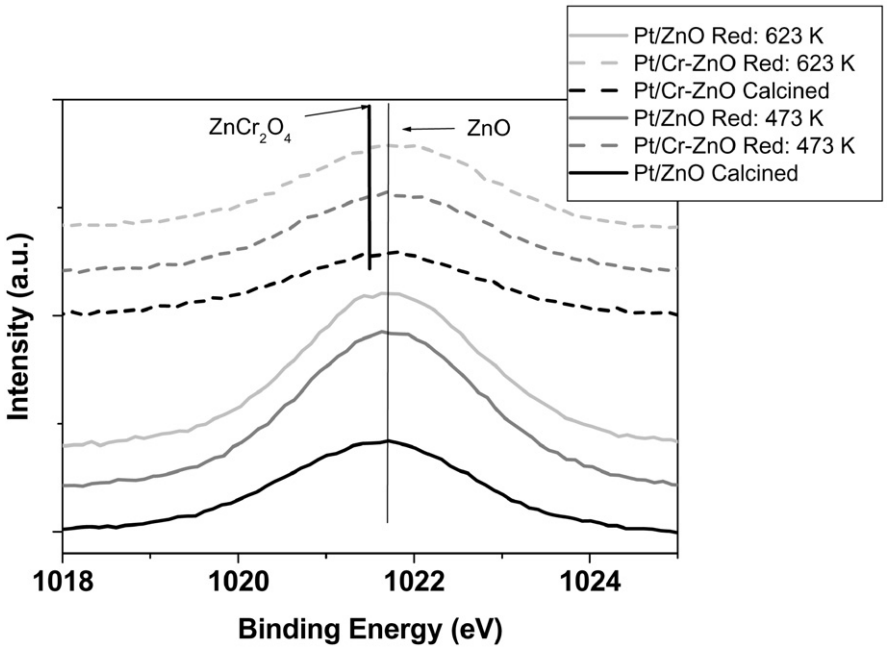

Fig. 6. Zn $2p_{3/2}$ core-level XPS spectra of the Pt/Cr–ZnO and Pt/ZnO after calcination and reduction treatments.

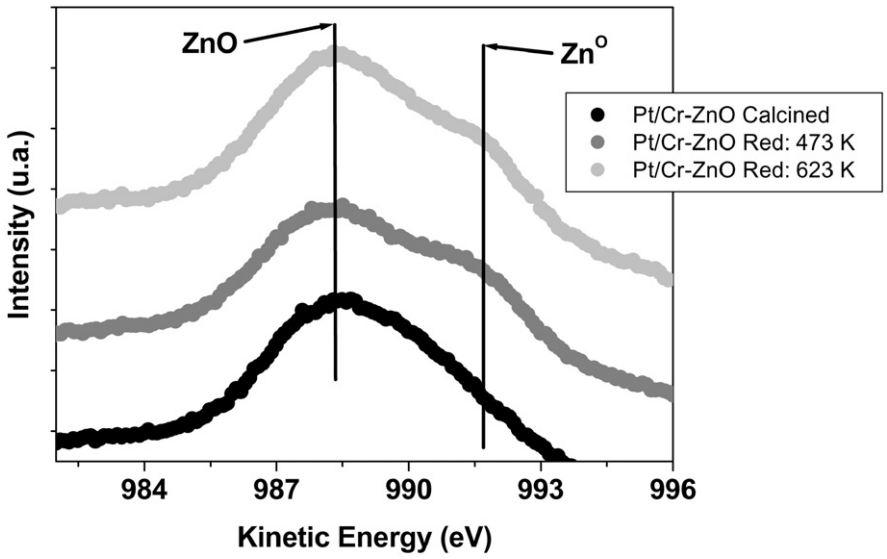

Fig. 7. Zn LMM Auger transition for Pt/Cr–ZnO after calcination and reduction treatments.

The BE of Zn $2p_{3/2}$ transition does not permit to discern the oxidation state of zinc. In the catalysts studied in this work, a single band appears centred at 1021.7 eV, which could be assigned to Zn(II) species (Fig. 6). The band is quite broad, this indicating the presence of zinc cations in different environments (ZnO, $Zn(OH)_2$, etc.). This assertion is consistent with the XPS O 1s data discussed above. The XPS Zn 2p spectra for the Pt/ZnO catalyst obtained after the reduction treatments are also shown in Fig. 6. Reduction at 473 K and at 623 K produced an insignificant shift in binding energy. However, the band widths are lower than that of the calcined sample, this probably being due to a lower influence by the Zn hydroxide feature. The XPS Zn 2p spectrum of calcined un-reduced Pt/Cr–ZnO showed a peak centred at 1021.7 eV, which is wider than that obtained with the Pt/ZnO catalyst. This indicates that the peak broadness is not only due to the presence of zinc hydroxide but, in this case, the Zn:Cr spinel structure located on the surface can also play its role [41]. However, it was not possible to distinguish between zinc species forming part of ZnO or $Zn(OH)_2$ and that forming $ZnCr_2O_4$.

The difficulty of assessing the oxidation state of zinc by XPS measurements is well recognized in the literature, as the binding energies of metallic and oxidised Zn species are very close. In this case, it is necessary to take into account the analysis of the Zn LMM Auger transition, which is more sensitive to oxidation state of zinc [42]. For both the Pt/ZnO and the Pt/Cr–ZnO catalysts, the Auger spectra showed the absence of metallic zinc in the calcined un-reduced catalysts (band centred at 988.1 eV, assigned to Zn(II) species). The reduction treatments resulted in a shoulder at a kinetic energy of 991.7 eV, attributed to metallic Zn (as an example, Fig. 7 shows the Zn LMM Auger [13,25] transition of catalyst Pt/Cr–ZnO after the different treatments). The XPS spectrum in the Cr $2p_{3/2}$ region (not shown) showed one peak at 576 eV, which is assigned to Cr(III) species [41,43–45].

Table 1
XPS characterisation of catalysts

	Reduction temperature (K)	Pt/(Cr + Zn) (at)	Cr/Zn (at)
Pt/Cr,ZnO	Calcined	0.160	0.082
	Red: 473 K	0.120	0.100
	Red: 623 K	0.131	0.160
Pt/ZnO	Calcined	0.040	–
	Red: 473 K	0.050	–
	Red: 623 K	0.072	–

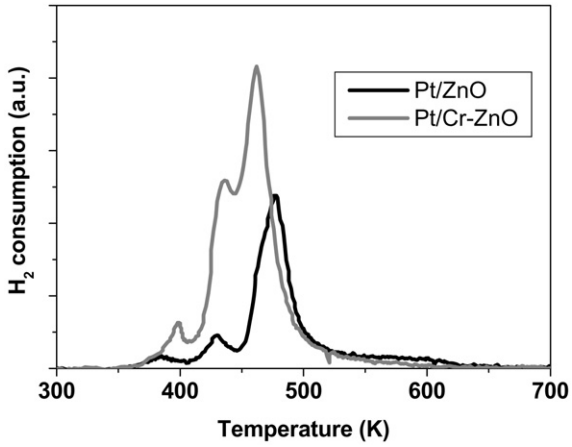

Fig. 8. TPR profiles of the Pt/Cr,ZnO and Pt/ZnO catalysts.

The XPS atomic ratios between the different components in the catalysts are shown in Table 1. In principle, the Pt/Zn ratio for the Pt/ZnO catalyst and the Pt/(Cr + Zn) ratio for the Pt/Cr–ZnO catalyst can be indicative of platinum dispersion [37,38,46,47]. The Pt/Zn XPS ratio in Pt/ZnO indicates a lower amount of surface Pt, i.e., larger particles, than the Pt/Cr–ZnO catalyst for both calcined and reduced catalysts (Table 1). These results agree with those from TEM analysis (Figs. 3 and 4). On the other hand, the atomic XPS Cr/Zn ratios in Pt/Cr–Zn increased with increasing the reduction temperature. This demonstrates that the reduction treatment produced segregation of chromium species towards the surface. This result has been previously reported in other studies carried out by Raman and XPS [41,43,45].

3.5. Temperature-programmed reduction

Fig. 8 shows the temperature-programmed reduction (TPR) profiles (H_2-consumption) for both catalysts. Both TPR profiles exhibit three peaks centred at 400, 435 and one between 440–480 K. The first hydrogen consumption at low temperature (400 K) is assigned to the reduction of oxidised Pt species to metallic Pt. The second reduction peak at 435 K is assigned to the breakdown of Pt–O–Zn entities formed upon calcination and reduction of oxy-chlorinated Pt species. The third peak, centred at around 460 K for Pt/Cr–ZnO catalysts, is assigned to the surface reduction of ZnO in close contact with the platinum particles. In the case of Pt/ZnO catalysts, this peak is shifted at higher temperatures (475 K), this indicating that the reduction temperature of the support has been increased. These results are consistent with those previously reported by Consonni et al. [14].

The main difference between both catalysts found in these TPR experiments was the amount of H_2 consumed. The Cr-containing catalyst showed larger hydrogen consumption, this indicating greater support reducibility. The distortion produced in the würzite structure by the presence of chromium cations favours the support reducibility.

Table 2
CO chemisorption data of catalysts reduced at 473 K and 623 K

	Reduction temperature (K)	CO uptake (μmol/g)	CO/Pt
Pt/Cr–ZnO	Red: 473 K	4.2	0.0160
	Red: 623 K	2.5	0.0100
Pt/ZnO	Red: 473 K	0.25	0.0010
	Red: 623 K	0.01	0.0004

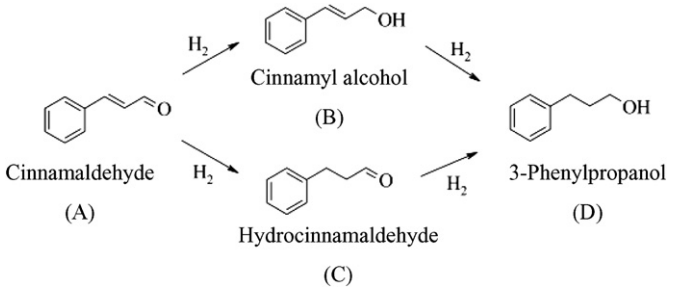

Fig. 9. Cinnamaldehyde hydrogenation reaction network.

3.6. CO chemisorption

The CO uptakes and the CO/Pt ratios obtained by CO chemisorption at room temperature after reduction at 473 and 623 K are reported in Table 2. The CO/Pt atomic ratios were very low for both catalysts after the two reduction treatments, in spite of the fact that the mean Pt particle size measured by TEM was very low. This is especially significant for catalyst Pt/ZnO. The CO uptake decreased after the reduction treatments, this being attributed to the influence of a strong metal–support interaction effect, as TEM studies revealed that no sintering of Pt particles had occurred. CO chemisorption should therefore not be used to calculate Pt particle sizes. Instead, it only will reflect the number of accessible Pt surface sites. A strong interaction of the metal with the support, the formation of alloy phase(s) between Pt and metallic Zn, and even the decoration of Pt particles by patches of support after reduction can be the origin of the low CO chemisorption capacity in these catalysts. In this way, in spite of the small size of the Pt particles present in the prepared catalysts, the amount of Pt atoms exposed seems to be very low.

3.7. Selective hydrogenation of cinnamaldehyde

Hydrogenation of cinnamaldehyde typically leads to three main reaction products, among which the desired one is cinnamylalcohol. The reaction scheme shown in Fig. 9 is rather simplified. Other by-products may appear, depending on the reaction conditions. For instance, the formation of acetals is typical for hydrogenations carried out over acidic catalysts. In accordance with Gallezot et al. [2], who reported solely the three main reaction products (**B**, **C**, **D**), there was no clear indication for other reactions. In the case of the catalysts studied in this work, the main reaction product found was cinnamylalcohol (unsaturated alcohol). Only a minor amount (about 5%) of other products was detected.

Fig. 10A shows the cinnamaldehyde concentration as function of time for the catalysts reduced at 473 K. Cinnamaldehyde was completely converted over both catalysts in less than 500 min, the Pt/Cr–ZnO catalyst being more active than Pt/ZnO. Fig. 10A also reports the initial rates, expressed in terms of a first order rate constant (min^{-1}). Fig. 10B shows the integral selectivity towards cinnamylalcohol (the amount of unsaturated alcohol present relative to the total amount of aldehyde converted) as function of the conversion of cinnamaldehyde, for the catalysts reduced at 473 K. Both samples catalysed selectively the formation

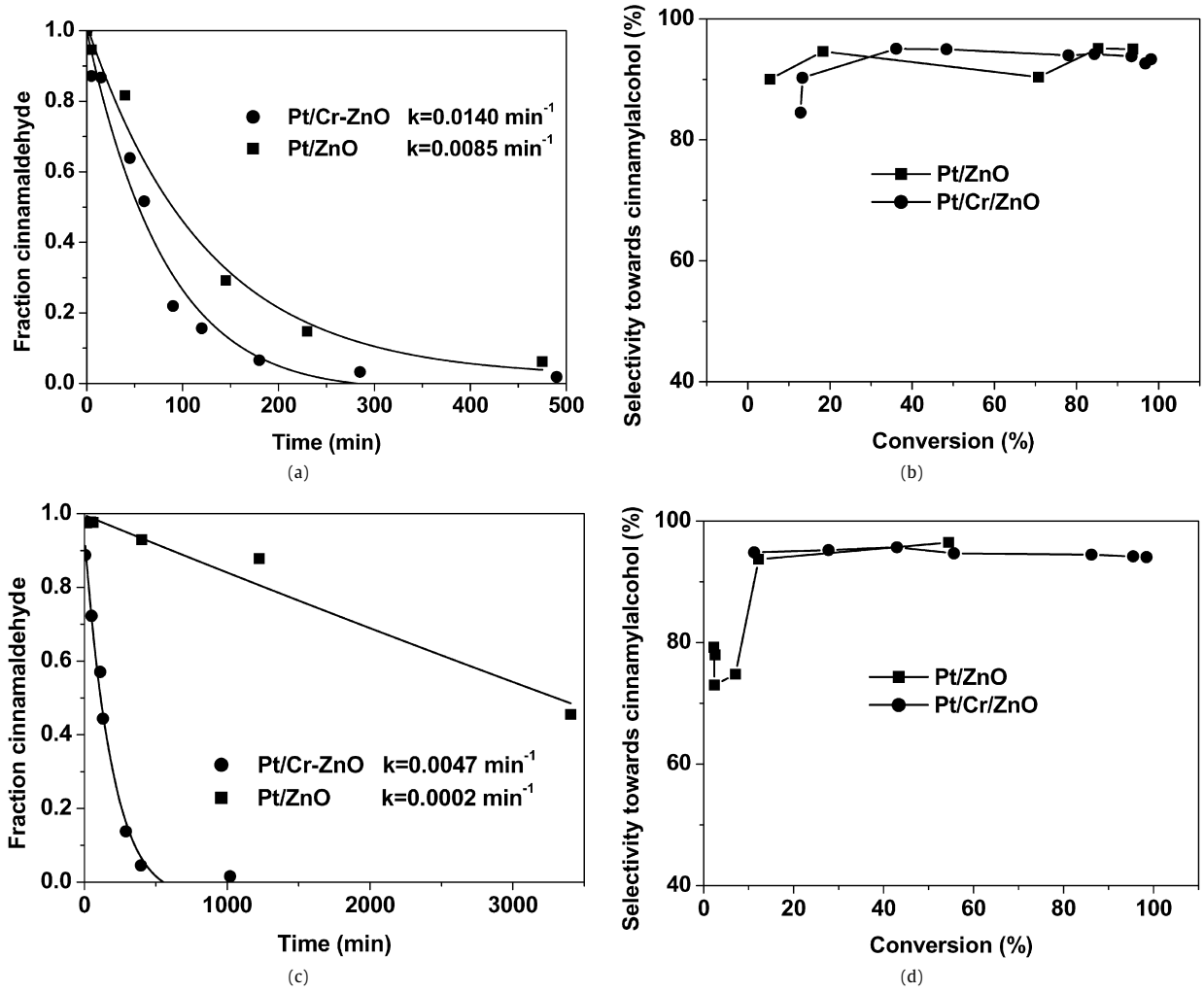

Fig. 10. Catalytic performance in the cinnamaldehyde hydrogenation (0.04 mol/L, 383 K and 7 MPa) after reduction at 473 K (a, b) and at 623 K (c, d): (a and c) cinnamaldehyde concentration as a function of time; (b and d) cinnamylalcohol selectivity as a function of conversion. First order rate constants are inserted.

of cinnamylalcohol (unsaturated alcohol), even up to high conversion. A small amount of hydrocinnamaldehyde was also detected (≈5%)

The catalytic performance of the catalysts reduced at 623 K is shown in Figs. 10C and 10D. The catalytic activities of both catalysts were lower than when reduced at 473 K, especially for catalyst Pt/ZnO. Reduction at 623 K produced a loss of active sites, as evidenced by CO chemisorption, which is attributed to a strong metal-support interaction effect as discussed above [14,23]. The selectivity towards the desired product (cinnamylalcohol) is very high for both catalysts (>95%) for conversions above 15% up to complete conversion of cinnamaldehyde (Fig. 10D).

Catalytic tests and characterisation results demonstrated that at the lowest reduction temperature (473 K) the extent of the metal–support interaction was adequate to generate active sites that catalysed the formation of cinnamylalcohol. However, reduction at 623 K caused the extensive coverage of active sites by the support (especially for the Pt/ZnO catalyst). This result agrees with those previously reported for this kind of catalysts where it was shown that the SMSI effect can take place even after reduction at temperatures at low as 473 K [23]. Chromium addition increased the reducibility of the support, thus increasing the amount of Zn^0. The increased amount of Zn^0 resulted in a higher probability of alloy formation and in an increase of the support's conductivity, what can induce a change in the electronic properties of the active phase. Furthermore, the loss of active sites is lower than in the Pt/ZnO catalyst.

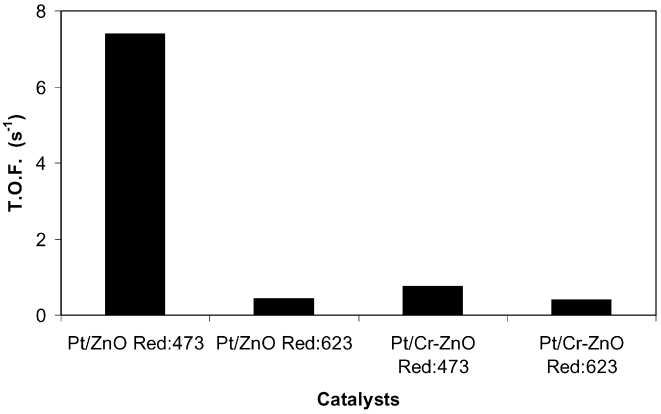

Fig. 11. Turnover frequencies for Pt/Cr,ZnO and Pt/ZnO catalysts reduced at 473 and 623 K in the cinnamaldehyde hydrogenation.

If the catalytic activities are represented as turn-over frequencies (TOF), some remarkable conclusions can be obtained. Fig. 11 shows the TOF for both catalysts after the two reduction temperatures used in this study, which were calculated using the CO chemisorption data (Table 2). After the reduction treatment at 473 K, the TOF value for Pt/ZnO was much higher than that for

Table 3
Best results reported recently for this reaction over Pt catalysts

Catalyst	Solvent	Reaction conditions	Conversion (%)	Selectivity (%)	Reference
Pt/montmorillonite	Isopropanol	298 K, 4.0 MPa	95	95	Szollosi et al., 1998 [52]
Pt/Na-montmorillonite	Ethanol	373 K, 7 MPa	65	80	Manikandan et al., 2007 [51]
PtRu/carbon nanotubes	Isopropanol	373 K, 2 MPa	80	93	Vu et al., 2006 [50]
Pt/Cr–ZnO	Isopropanol	383 K, 7 MPa	100	96	This work

Pt/Cr–ZnO. This indicates that the active sites formed in Pt/ZnO after this reduction treatment at low temperature are much more active. For Pt/Cr–ZnO, the number of active sites is higher and, thus, the overall activity is higher, but the intrinsic activity of the active sites is lower. However the TOF values are similar after reduction treatment at 623 K. This may be ascribed to different factors. On one hand, the surface segregation of chromium cations after the reduction treatments seems to avoid the migration of patches of the ZnO support over the metal particles and, consequently, the number of active sites remains higher. Furthermore, chromium addition enhances the support reducibility producing an increase in the amount of metallic zinc, which favours the formation of alloy phases, this also affecting the catalytic activity [21,48,49].

The results found have special relevance in terms of selectivity. It has been recently reported that this kind of catalysts show high activity and selectivity towards the production of the unsaturated alcohol [23] in the vapour phase selective hydrogenation of crotonaldehyde. But the use of vapour phase reaction limits their industrial applications. Thereby, it has been found that their good catalytic properties are kept also when they are used in the liquid phase and with a complex reaction such as the selective hydrogenation of cinnamaldehyde. When the results obtained with these catalysts are compared with those recently reported for supported platinum catalysts, it can be seen that these catalysts present the best selectivity found without the use additives to the reaction medium (Table 3) [50–52]. The high selectivity is attributed to the electronic donating interaction of the metallic zinc to the platinum, this lowering the interaction of the olefinic double bond of the aldehyde with the catalyst [11,14].

4. Conclusions

The addition of Cr(III) cations to ZnO used as support for Pt catalysts in the selective hydrogenation of cinnamaldehyde generated several modifications both in the support and in the catalyst behaviour: (i) $ZnCr_2O_4$ spinel (mixed oxide) was generated; (ii) the textural properties (larger surface area and resistance against sintering) were improved; (iii) the presence of chromium favoured the reducibility of ZnO; (iv) Pt dispersion was increased. The catalytic performance was enhanced with these modifications, resulting in a very active and selective catalyst. About 95% selectivity towards cinnamylalcohol was obtained up to complete conversion. This enhancement is ascribed to a favourable metal–support interaction induced by chromium addition and the higher reducibility of ZnO. The reduction temperature controls both the catalytic activity and the selectivity. After reduction treatment at low temperature (473 K), a very active and selective (90–95%) catalyst was obtained, while reduction at high temperature (623 K) decreased the activity, especially for the Cr-free catalyst, but the selectivity was slightly improved to 95%.

Acknowledgments

This work was supported from Ministerio de Educación y Ciencia, Spain (Projects BQU2003-06150 and NAN2004-09267-C03) and European Commission (Contract No. NMP3-CT2004-500895 'InsidePores' Network of Excellence).

References

[1] M. De Bruyn, S. Coman, R. Bota, V.I. Parvulescu, D. De Vos, P.A. Jacobs, Angew. Chem. 42 (2003) 5333.
[2] P. Gallezot, D. Richard, Rev.-Sci. Eng. 40 (1998) 81.
[3] A. Corma, L.T. Nemeth, M. Renz, S. Valencia, Nature 412 (2001) 423.
[4] A. Corma, M.E. Comine, L.T. Nemeth, S. Valencia, J. Am. Chem. Soc. 124 (2002) 3194.
[5] A. Corma, M.E. Domine, S. Valencia, J. Catal. 215 (2003) 294.
[6] A. Corma, H. Garcia, Chem. Rev. 103 (2003) 4307.
[7] J. Jeak, J.E. Germain, J. Catal. 65 (1980) 133.
[8] A. Giroir-Fendler, D. Richard, P. Gallezot, Stud. Surf. Sci. Catal. 41 (1988) 171.
[9] J.C.S. Wu, T.-S. Cheng, C.-L. Lai, Appl. Catal. A Gen. 314 (2006) 233.
[10] T.B.L. Marinelli, V. Ponec, J. Catal. 156 (1995) 51.
[11] J.L. Margitfalvi, I. Borbáth, M. Hegedus, A. Tompos, Catal. A Gen. 229 (2002) 35.
[12] J.C. Serrano-Ruiz, A. Sepúlveda-Escribano, F. Rodríguez-Reinoso, J. Catal. 246 (2007) 158.
[13] J. Silvestre-Albero, J.C. Serrano-Ruiz, A. Sepúlveda-Escribano, F. Rodríguez-Reinoso, Appl. Catal. A Gen. 292 (2005) 244.
[14] M. Consonni, D. Jokic, D.Y. Murzin, R. Touroude, J. Catal. 188 (1999) 165.
[15] P. Gallezot, A. Giroir-Fendler, D. Richard, Catal. Lett. 5 (1990) 164.
[16] D.G. Blackmond, R. Oukaci, B. Blanc, P. Gallezot, J. Catal. 131 (1991) 401.
[17] A. Giroir-Fendler, D. Richard, P. Gallezot, Stud. Surf. Sci. Catal. 41 (1988) 171.
[18] M.L. Toebes, T.A. Nijhuis, J. Hájek, J.H. Bitter, A.J. Van Dellen, D. Murzin, K.P. De Jong, Chem. Eng. Sci. 60 (2005) 5682.
[19] M.L. Toebes, Y. Zhang, J. Hájek, T. Nijhuis, J.B. Bitter, A. Jos Van Dillen, D.Y. Murzin, D.C. Koningsberger, K.P. De Jong, J. Catal. 226 (2004) 215.
[20] A. Dandekar, M.A. Vannice, J. Catal. 183 (1998) 344.
[21] M.A. Vannice, Top. Catal. 4 (1997) 241.
[22] A. Huidobro, A. Sepúlveda-Escribano, F. Rodríguez-Reinoso, J. Catal. 212 (2002) 94.
[23] E.V. Ramos-Fernández, A. Sepúlveda-Escribano, F. Rodríguez-Reinoso, DOI: 10.1016/j.catcom.2007.11.010.
[24] A. Sepúlveda-Escribano, F. Coloma, J. Silvestre-Albero, F. Rodríguez-Reinoso, Appl. Catal. A Gen. 304 (2006) 159.
[25] J. Silvestre-Albero, F. Rodríguez-Reinoso, A. Sepúlveda-Escribano, J. Catal. 210 (2002) 127.
[26] A. Sepúlveda-Escribano, F. Coloma, F. Rodríguez-Reinoso, J. Catal. 178 (1998) 649.
[27] A. Sepúlveda-Escribano, J. Silvestre-Albero, F. Coloma, F. Rodríguez-Reinoso, Stud. Surf. Sci. Catal. 130 (2000) 1013.
[28] S. Bernal, M.A. Cauqui, G.A. Cifredo, J.M. Gatica, C. Larese, J.A. Pérez-Omil, Catal. Today 29 (1996) 77.
[29] B. Campo, M. Volpe, S. Ivanova, R. Touroude, J. Catal. 242 (2006) 162.
[30] K. Liberková, L. Cerveny, R. Touroude, Res. Chem. Intermed. 26 (2003) 609.
[31] K. Liberková, R. Touroude, J. Mol. Catal. A Chem. 180 (2002) 221.
[32] M. Ohta, Y. Ikeda, A. Igarashi, Appl. Catal. A Gen. 258 (2003) 153.
[33] D.A. Shirley, Phys. Rev. B 5 (1972) 4709.
[34] R.B. Kale, H. Yung-Jung, L. Yi-Feng, L. Shih-Yuan, Solid State Commun. 142 (2007) 302.
[35] J. Wang, Y. Wang, S. Xie, M. Qiao, H. Li, K. Fan, Appl. Catal. A Gen. 272 (2004) 29.
[36] X. Wang, S. Yang, J. Wang, M. Li, X. Jiang, G. Du, X. Liu, R.P.H. Chang, J. Cryst. Growth 19 (2001) 123.
[37] J.A. Rodríguez, M. Kuhn, J. Chem. Phys. 102 (1995) 4279.
[38] A. Sepúlveda-Escribano, J.C. Serrano-Ruiz, G.W. Huber, M.A. Sanchez-Castillo, J.A. Dumesic, F. Rodríguez-Reinoso, J. Catal. 241 (2006) 378.
[39] P. Concepción, A. Corma, J. Silvestre-Albero, V. Franco, J.Y. Chane-Ching, J. Am. Chem. Soc. 126 (2004) 5523.
[40] L. Jing, D. Wang, B. Wang, S. Li, B. Xin, H. Fu, J. Sun, J. Mol. Catal. A Chem. 244 (2006) 193.
[41] W.E. Epling, G.B. Hoflund, D.M. Minahan, J. Catal. 175 (1998) 175.
[42] J. Silvestre-Albero, A. Corma, A. Sepúlveda-Escribano, F. Rodríguez-Reinoso, Appl. Catal. A Gen. 304 (2006) 159.

[43] W.E. Epling, G.B. Hoflund, W.M. Hart, D.M. Minahan, J. Catal. 172 (1997) 13.
[44] B. Liu, M. Terano, J. Mol. Catal. A Chem. 172 (2001) 227.
[45] W.E. Epling, G.B. Hoflund, W.M. Hart, D.M. Minahan, J. Catal. 169 (1997) 438.
[46] F.P.J.M. Kerkhof, J.A. Moulijn, J. Phys. Chem. 83 (1979) 1612.
[47] A. Huidobro, A. Sepúvelda-Escribano, F. Rodríguez-Reinoso, J. Catal. 121 (2002) 94.
[48] P. Claus, Top. Catal. 5 (1998) 51.
[49] V. Ponec, Appl. Catal. A Gen. 149 (1997) 27.
[50] H. Vu, F. Gonçalves, R. Philippe, E. Lamouroux, M. Corrias, Y. Kihn, D. Plee, P. Kalck, P. Serp, J. Catal. 240 (2006) 18.
[51] D. Manikandan, D. Divakar, T. Sivakumar, Catal. Commun. 8 (2007) 1781.
[52] G. SzöllöSi, B. Török, L. Baranyi, M. Bartók, J. Catal. 179 (1998) 619.